

The divergence of neighboring magnetic field lines and fast-particle diffusion in strong magnetohydrodynamic turbulence, with application to thermal conduction in galaxy clusters

Jason Maron and Benjamin D. G. Chandran
*Department of Physics and Astronomy, University of Iowa**

Eric Blackman
Department of Physics and Astronomy, University of Rochester†

Using direct numerical simulations, we calculate the rate of divergence of neighboring magnetic field lines in different types of strong magnetohydrodynamic turbulence. In the static-magnetic-field approximation, our results imply that tangled magnetic fields in galaxy clusters reduce the electron diffusion coefficient and thermal conductivity by a factor of $\sim 5 - 10$ relative to their values in a non-magnetized plasma.

PACS numbers: 52.25.Fi, 52.55.Jd, 98.62.Ra, 98.62.En

The diffusion of fast particles in turbulent magnetized plasmas is important for fusion experiments, cosmic-ray propagation, and thermal conduction in galaxy-cluster plasmas [1, 2, 3, 4, 5, 6, 7, 8, 9, 10, 11, 12, 13]. We consider particle diffusion in a static magnetic field, which is a reasonable first approximation for particles moving much faster than the $\mathbf{E} \times \mathbf{B}$ velocity of field lines. The effects of turbulent bulk motions and field evolution have recently been considered by [13, 14].

We consider magnetic fluctuations that possess an inertial range extending from an outer scale l_B to a much smaller inner scale l_d with the magnetic energy dominated by scales $\sim l_B$. Except where specified, the discussion focuses on the case in which there is no mean magnetic field pervading the plasma. If a particle is tied to a single field line and travels a distance $l \gg l_B$ along the static magnetic field, it takes $\sim l/l_B$ random-walk steps of length l_B , resulting in a mean-square three-dimensional displacement of

$$\langle(\Delta x)^2\rangle = \alpha l_B l, \quad (1)$$

where α is a constant of order unity. The values of α for the turbulence simulations used in this paper are listed in table I. When there is a mean field \mathbf{B}_0 comparable to the rms field, $\langle(\Delta x)^2\rangle$ in equation (1) is interpreted as the mean-square displacement perpendicular to \mathbf{B}_0 . If the particle's motion along the field is diffusive with diffusion coefficient D_{\parallel} , then

$$l \sim \sqrt{D_{\parallel} t}, \quad (2)$$

and [15, 16]

$$\langle(\Delta x)^2\rangle \propto t^{1/2}, \quad (3)$$

indicating subdiffusion [$D \equiv \lim_{t \rightarrow \infty} \langle(\Delta x)^2\rangle/6t \rightarrow 0$].

In fact, a particle is not tied to a single field line. After traveling a short distance along the field, field gradients and scattering cause a particle to take a step comparable to its gyroradius ρ across the magnetic field, from its initial field line, F1, to a new field line, F2. If the particle were to follow F2, it would separate from F1 because neighboring field lines tend to diverge. We call z_s the distance the particle would have to

follow F2 before separating from F1 by a distance l_B . (A particle typically separates from its initial field line by a distance l_B after traveling a distance slightly less than z_s since it drifts across the field continuously, but we ignore this effect in this paper.)

If a particle “takes a random step” of length mz_s along the magnetic field, where m is a constant of order a few, reverses direction, and then takes another random step of length mz_s back along the field, it doesn't return to its initial point. Part of the second step retraces part of the first step, but the remainder is uncorrelated from the first step. This loss of correlation leads to a Markovian random walk [8, 14]. When $mz_s \gg l_B$, a single random step corresponds to a 3D displacement of

$$(\Delta x)^2 \sim \alpha m z_s l_B. \quad (4)$$

When $mz_s \gg \lambda$, where λ is the Coulomb mean free path, a single step takes a time

$$\Delta t \sim \frac{m^2 z_s^2}{D_{\parallel}}. \quad (5)$$

When mz_s is only moderately greater than l_B or λ , equations (4) and (5) remain approximately valid. During successive random steps, a particle will find itself in regions of differing magnetic shear, and thus z_s will vary. The diffusion coefficient is given by $D = \langle(\Delta x)^2\rangle/6\langle\Delta t\rangle$ where $\langle \dots \rangle$ is an average over a large number of steps [17]. Ignoring factors of order unity,

$$D \sim D_{\parallel} \frac{l_B}{L_S} \quad (6)$$

as in [8, 14, 15], with

$$L_S = \frac{\langle z_s^2 \rangle}{\langle z_s \rangle}. \quad (7)$$

If there is a mean magnetic field comparable to the fluctuating field, equation (6) is recovered provided D is replaced by D_{\perp} , the coefficient of diffusion perpendicular to the mean field.

We treat field-line separation in a static field using magnetic-field data obtained from four direct numerical simulations of incompressible MHD turbulence. Key simulation

parameters are given in table I. The numerical method is described in [18]. Each simulation uses Newtonian viscosity ν and resistivity η and is run until a statistical steady state is reached. In simulations A1 and A2, the mean magnetic field is zero, and the initial magnetic field is dominated by large-scale fluctuations containing 10% of the maximum possible magnetic helicity. Turbulent fluctuations are sustained by non-helical random forcing of the velocity field, and the magnetic Prandtl number $P_m \equiv \nu/\eta$ equals 1. These simulations reach a statistical steady state with Kolmogorov-like kinetic and magnetic power spectra. In simulation B, $P_m = 75$ and the field is amplified from an initially weak seed magnetic field by turbulent velocities sustained by non-helical random forcing. When the dynamo growth of the magnetic field saturates, the magnetic field is dominated by fluctuations on scales much smaller than the dominant velocity length scale, as in the simulations of [19]. In simulation D, $P_m = 1$ and the field is amplified from an initially weak seed magnetic field by turbulent velocities sustained by maximally helical random forcing. When the dynamo growth of the magnetic field saturates, the dominant magnetic field length scale is comparable to the dominant velocity length scale, as in the simulations of [20]. “Simulation” A2_{rp} is obtained by assigning each Fourier mode in simulation A2 a random phase without changing the mode’s amplitude. In simulations A1, A2, A2_{rp}, and D we set π/l_B equal to the maximum of $kE_b(k)$, where $E_b(k)$ is the power spectrum of the magnetic field [the total magnetic energy is $\int E_b(k)dk$]. In simulation B we take π/l_B to be the maximum of $kE_v(k)$, where $E_v(k)$ is the power spectrum of the velocity field. We set π/l_d equal to the maximum of $k^3 E_b(k)$.

Simulation	Grid points	$\frac{\delta B}{ \langle \mathbf{B} \rangle }$	H_m	l_B/l_d	α	P_m
A1	256 ³	∞	0.1	23	2.4	1
A2	512 ³	∞	0.1	50	2.4	1
B	256 ³	∞	0	90	0.2	75
D	256 ³	∞	0.8	30.7	1.9	1

TABLE I: $\delta B/|\langle \mathbf{B} \rangle|$ is the ratio of the rms fluctuating field to the mean field, H_m is the magnetic helicity divided by the maximum possible magnetic helicity at that level of magnetic energy, l_B/l_d is the ratio of outer scale to inner scale, and α is the coefficient in equation (1).

We take a snapshot of the magnetic field in each simulation and introduce 2,000 pairs of field-line tracers whose initial separation \mathbf{r}_0 is perpendicular to the local field. We use linear interpolation to obtain the magnetic field between grid points and employ second-order Runge-Kutta to integrate field-lines. To improve the statistics in simulation A1, we use 2,000 field lines in each of seventeen snapshots of the field separated in time by an interval $0.4l_B/u$, where u is the rms velocity. In simulations A2 and A2_{rp}, we use 20,000 field lines in each of five snapshots of the magnetic field separated in time by an interval $0.2l_B/u$. We iteratively reduce the length step in the field-line integrations to achieve convergence.

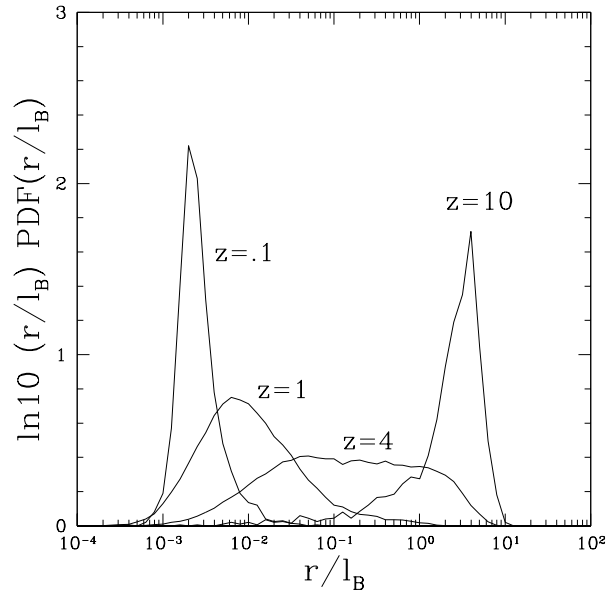


FIG. 1: The probability distribution function of field-line separations in simulation A1 with $r_0 = 2^{-9}l_B$.

The probability distribution function (PDF) of field-line separations in simulation A1 for $r_0 = 2^{-9}l_B$ is plotted in figure 1 for different values of the distance z a field-line pair is followed along the magnetic field. [The probability is per unit $\log_{10}(r/l_B)$, so that the probability that r lies in some interval is proportional to the area under the plotted curves.] The PDF is highly non-Gaussian, and the tail of the distribution dominates the growth of $\langle r \rangle$ when $l_d < \langle r \rangle < l_B$. The maximum kurtosis $\langle r^4 \rangle / \langle r^2 \rangle^2$ is ~ 500 and occurs for $z \simeq 0.2$. We find that decreasing r_0 increases the maximum kurtosis.

The growth of $\langle r \rangle$ with z in simulation A1 is shown in figure 2 for several values of r_0 . There are three stages of growth similar to those described in previous theoretical treatments of field-line divergence [10, 11]: (1) an initial stage of exponential growth when $r_0 \ll l_d$, (2) approximate power-law growth with $r \propto z^a$ for $\langle r \rangle \ll l_B$, and (3) $\langle r \rangle \propto z^{1/2}$, for $\langle r \rangle > l_B$. However, some aspects of our results differ from previous studies. Within a single simulation, a increases with decreasing r_0 , which is probably related to the increasing prominence of the tail of the PDF as r_0 is decreased. In addition, stage 2 with $\langle r \rangle \propto z^a$ begins for $\langle r \rangle < l_d$, perhaps because the field-line pairs with largest r , which dominate the growth of $\langle r \rangle$, satisfy $r > l_d$ before $\langle r \rangle > l_d$.

We seek to test the qualitative prediction of [9, 10, 11] that $\langle z_s \rangle$ and L_S asymptote to a value of order a few l_B as r_0 is decreased towards l_d in the large- l_B/l_d limit. In figure 3, we plot $\langle z_s \rangle$ for simulation A1 and simulation A2. The lower-resolution data of simulation A1 suggest the scaling $\langle z_s \rangle \propto \ln(l_B/r_0)$ for $l_d < r_0 < 0.25l_B$, in contradiction to the theoretical treatments. On the other hand, for simulation A2, the curve through the data is concave downward for $l_d < r_0 < l_B$.

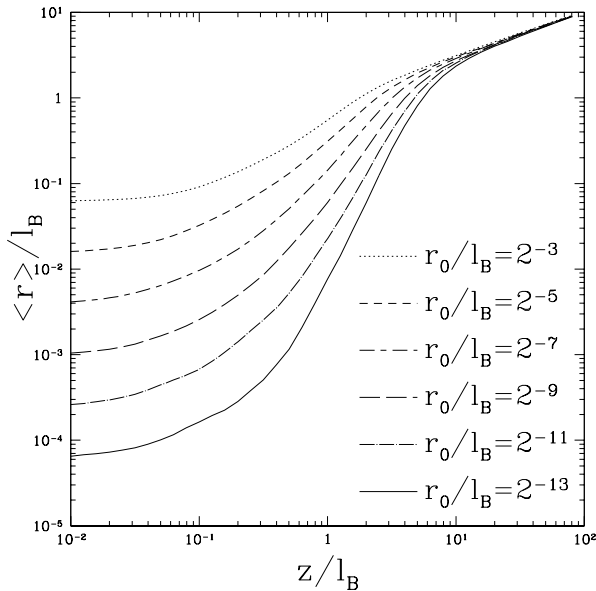


FIG. 2: Mean field-line separation $\langle \Delta r \rangle$ as a function of distance l travelled along the magnetic field in simulation A for different values of r_0 .

Moreover, figure 3 shows that the simulation A1 data, and probably also the A2 data, have not converged to the high-Reynolds-number values of $\langle z_s \rangle$ for $l_B/16 < r_0 < l_B$, values of r_0 that are within the inertial ranges (l_d to l_B) of both simulations. Also, the slope $d\langle z_s \rangle / d(\ln(l_B/r_0))$ for both $r_0 < l_d$ and $r_0 < l_B/10$ decreases significantly when l_B/l_d is doubled. A comparison of the data for A1 and A2 thus suggests that in the large- l_B/l_d limit $\langle z_s \rangle$ asymptotes to a value of order several l_B as r_0 is decreased towards l_d , as in [9, 10, 11]. The same comments apply to the data for L_S , which are plotted in figure 4.

We note that for $r_0 = l_B$, $\langle z_s \rangle$ and L_S are by definition 0. The numerical-simulation data points that appear to be plotted above $l_B/r_0 = 1$ actually correspond to r_0 just slightly smaller than l_B , indicating that $\langle z_s \rangle$ and L_S are discontinuous at $r_0 = l_B$ in the numerical simulations. The reason is that for r_0 just slightly less than l_B , some fraction of the field line pairs are initially converging and must be followed a significant distance before they start to diverge.

The thermal conductivity κ_T in galaxy-cluster plasmas scales approximately like the diffusion coefficient of thermal electrons [15, 16]. For clusters, $l_B/l_d \simeq l_B/\rho_i \simeq 10^{13}$, where ρ_i is the proton gyroradius [21]. In the large- l_B/l_d limit, the numerical simulations and theoretical models indicate that L_S asymptotes to a value of order several l_B as r_0 is decreased towards l_d , and L_S is not expected to increase appreciably as r_0 is further decreased from $l_d = \rho_i$ to ρ_e . Thus, $L_S(\rho_e) \simeq L_S(l_d)$. We take simulations A1 and A2 to be our best models of a galaxy-cluster magnetic field. We find that $L_S(l_d) \simeq 11l_B$ in A1 with $l_B/l_d = 23$, and $L_S(l_d) \simeq 10 - 11l_B$

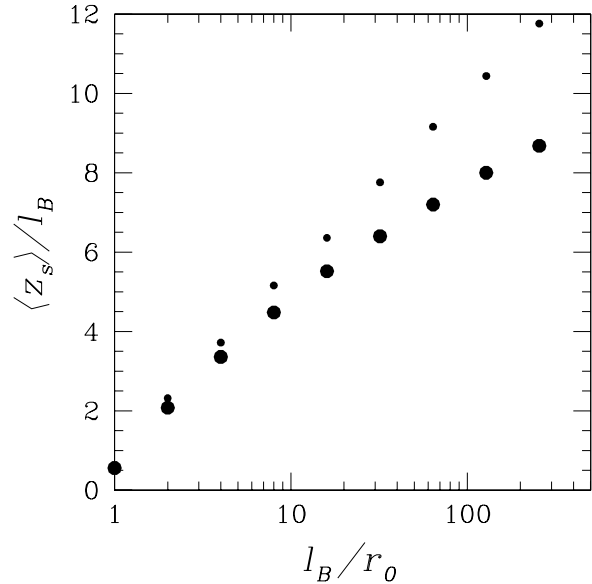


FIG. 3: The average distance $\langle z_s \rangle$ that a field-line pair must be followed before separating by a distance l_B as a function of initial field-line separation r_0 for simulations A1 (small circles) and A2 (large circles).

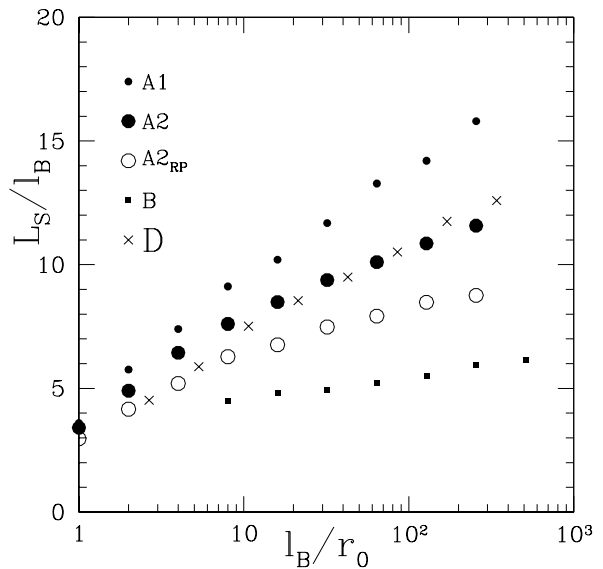


FIG. 4: The dependence of L_S on r_0 .

in A2 with $l_B/l_d = 50$. If l_B is redefined so that $2\pi/l_B$ (instead of π/l_B) equals the maximum of $kE_b(k)$, then $L_S(l_d) \simeq 7l_B$ in A1 and $L_S(l_d) \simeq 6.5l_B$ in A2[14]. Since the definition of l_B contains an arbitrary constant of order unity, it is not clear which of the two definitions leads to the more accurate prediction of κ_T . Given this uncertainty, extrapolating these re-

sults to the large- l_B/l_d limit suggests that $L_S(l_d) \sim 5 - 10l_B$ in intracluster plasmas. Diffusion along the magnetic field can be suppressed by magnetic mirrors [8, 12] and wave pitch-angle scattering [22], but in clusters the Coulomb mean free path is sufficiently short that neither of these effects is very important. [11, 14] Thus, the parallel diffusion coefficient of thermal electrons is comparable to the thermal-electron diffusion coefficient in a non-magnetized plasma, D_0 . In the static-magnetic-field approximation, equation (6) thus implies that $D/D_0 \sim 0.1 - 0.2$ for thermal electrons in intracluster plasmas, and that κ_T is reduced by a factor of $\sim 5 - 10$ relative to the Spitzer thermal conductivity κ_S of a non-magnetized plasma. Heating of intracluster plasma from thermal conduction with $\kappa_T \sim 0.1 - 0.2\kappa_S$ would be sufficient to balance radiative cooling in some but not all clusters [23, 24]. More work is needed to determine the validity of the static-field approximation in clusters, to determine the factors of order unity that have been neglected in our phenomenological treatment of thermal conduction, and to clarify the effects of turbulent diffusion and turbulent resistivity on heat conduction in strong MHD turbulence.

We thank Steve Cowley and Alex Schekochihin for valuable discussions. This work was supported by NSF grant AST-0098086 and DOE grants DE-FG02-01ER54658 and DE-FC02-01ER54651 at the University of Iowa, with computing resources provided by the National Partnership for Advanced Computational Infrastructure and the National Center for Supercomputing Applications.

[†] Electronic address: blackman@pas.rochester.edu

- [1] A. C. Fabian, *Annu. Rev. Astron. Astrophys.*, **32**, 277 (1994)
- [2] J. Binney and L. L. Cowie, *Astrophys. J.*, **247**, 464 (1981)
- [3] R. Rosner and W. H. Tucker, *Astrophys. J.*, **338**, 761 (1989)
- [4] P. C. Tribble, *Mon. Not. R. Astr. Soc.*, **238**, 1247 (1989)
- [5] E. Chun and R. Rosner, *Astrophys. J.*, **408**, 678 (1993)
- [6] L. Tao, *Mon. Not. R. Astr. Soc.*, **275**, 965 (1995)
- [7] S. Pistinner and G. Shaviv, *Astrophys. J.*, **459**, 147 (1996)
- [8] B. D. G. Chandran and S. Cowley, *Phys. Rev. Lett.*, **80**, 3077 (1998)
- [9] J. Jokipii, *Astrophys. J.*, **183**, 1029
- [10] J. Skilling, I. McIvor, and J. A. Holmes, *MNRAS*, *167*, 87P (1974)
- [11] R. Narayan, M. Medvedev, *Astrophys. J.*, **562**, 129 (2001)
- [12] L. Malyskin, and R. Kulsrud, *Astrophys. J.*, 549, 402
- [13] A. Gruzinov, astro-ph/0203031 (2002)
- [14] B. D. G. Chandran, and J. Maron, *Astrophys. J.*, accepted
- [15] A. B. Rechester and M. N. Rosenbluth, *Phys. Rev. Letters*, **40**, 38 (1978)
- [16] J. A. Krommes, C. Oberman, and R. G. Kleva, *J. Plasma Physics*, **30**, 11 (1983)
- [17] S. Chandrasekhar, *Rev. Mod. Phys.*, **15**, 1 (1943)
- [18] J. Maron and P. Goldreich, *Astrophys. J.*, **554**, 1175 (2001)
- [19] J. Maron, S. Cowley, and J. McWilliams, accepted for publication in *Astrophys. J.*
- [20] J. Maron, and E. Blackman, *Astrophys. J.*, **556L**, 41 (2002)
- [21] E. Quataert, *Astrophys. J.*, **500**, 978 (1998)
- [22] S. Pistinner, and D. Eichler, *Mon. Not. R. Astr. Soc.*, **301**, 49 (1998)
- [23] A. C. Fabian, astro-ph/0210150
- [24] N. Zakamska, and R. Narayan, R., *Astrophys. J.* (2003), in press

* Electronic address: jason-maron@uiowa.edu, benjamin-chandran@uiowa.edu